Materials Science & Engineering A 609 (2014) 147–153

Contents lists available at ScienceDirect

Materials Science & Engineering A

journal homepage: www.elsevier.com/locate/msea

Effects of deep cryogenic treatment and low-temperature aging on the mechanical properties of friction-stir-welded joints of 2024-T351 aluminum alloy

Ji Wang [a,b], Ruidong Fu [a,b,*], Yijun Li [a,b], Jianfeng Zhang [a,b]

[a] State Key Laboratory of Metastable Materials Science and Technology, Yanshan University, Qinhuangdao, Hebei 066004, PR China
[b] College of Materials Science and Engineering, Yanshan University, Qinhuangdao, Hebei 066004, PR China

ARTICLE INFO

Article history:
Received 16 February 2014
Received in revised form
14 April 2014
Accepted 17 April 2014
Available online 29 April 2014

Keywords:
Aluminum alloys
Friction stir welding
Deep cryogenic treatment
Low-temperature aging
Tensile properties

ABSTRACT

Low-temperature aging treatments at 120 °C for 8 h, with and without deep cryogenic pretreatments, were conducted for friction-stir-welded joints of 2024-T351 aluminum alloys. The microstructures and mechanical properties of the welded joints after the above treatments were investigated. Two obvious soft zones were found to be located at the retreating and advancing sides of the heat-affected zone (HAZ) in the as-welded joint. After a single low-temperature aging treatment (LTA), the soft regions close to the base metal in the HAZ almost vanished, while the soft regions close to the thermal-mechanical-affected zone were not significantly affected. Moreover, tensile fracture occurred along the segregation bands of the precipitates in the nugget zone (NZ). This resulted in a decrease in the elongation of the as-welded joint from 74% to 38% that of the base metal. After low-temperature aging with a deep cryogenic pretreatment at 77 K, the features of the soft zones were similar to those in the case of the single LTA, but the tensile fracture at the segregation bands in the NZ was inhibited. Consequently, the elongation of the joints improved along with an increase in tensile strength. The possible mechanisms related to the improvement of tensile properties of the joints were discussed.

1. Introduction

Friction stir welding (FSW) is a solid-state joining technique that has been successfully applied to the joining of high-strength aluminum alloys, which are difficult to weld by fusion welding methods [1]. Based on the features of the microstructure, several different zones were clarified along the transverse direction of the FSW joint, such as the nugget zone (NZ), Thermo Mechanically affected zone (TMAZ), and heat-affected zone (HAZ). Severe plastic deformation and high temperatures in the NZ and partial TMAZ result in grain refinement, texture development, and dissolution or re-precipitation of precipitates. In the HAZ, only a slight growth of the grain, and dissolution or coarsening of the precipitates occur. The problem related to these variations in the microstructure is the softening of the FSW joints. For example, Jones et al. found that there were two minima hardness zones in the HAZ of FSW joints for the 2024-T351 aluminum alloy. One minima was close to the TMAZ, attributable to the coarsening and over-aging of the *S* phase particles, and the other was close to the outer edge of the HAZ, attributable to the dissolution of very fine *S* phase particles [2]. The existence of the soft zone not only degrades the strength but also elongation of the joints. Therefore, many studies have been conducted to attempt the elimination of such soft regions by manipulating the thermal boundary conditions of the welded joint [3–5]. For example, Hassan et al. [3] found that for a given travel speed, the hardness values of NZ is positively proportional to the rotational speed of the tool. Reynolds et al. [4] found that the softening in HAZ of FSW aluminum alloy joint can be reduced by decreasing the exposed time at temperature of around 350 °C. Fu et al. [5] effectively restricted the softening in the FSW joint of 2024 aluminum alloy by using the parameter combination of high rotational speed (1500 rpm) and travel speed (1000 mm/min).

In addition, some researchers have attempted to restrict softening in the FSW joint by using external forced cooling [6–9]. For example, Upadhyay et al. [6] and Fratini et al. [7] found that water cooling resulted in higher strength and ductility of FSW joints. Detailed researches on FSW in air, cold water (approximately 8 °C), and hot water (about 90 °C) for a 7050 aluminum alloy was conducted by Fu et al. [8]. The results showed that the mechanical property of the FSW joint welded in hot water was the best among the welded joints tested. As mentioned above, either the optimization of the thermal conditions or external cooling methods

* Corresponding author at: State Key Laboratory of Metastable Materials Science and Technology, Yanshan University, Qinhuangdao, Hebei 066004, PR China. Tel.: +86 335 858 7046; fax: +86 335 807 4545.
E-mail address: rdfu@ysu.edu.cn (R. Fu).

http://dx.doi.org/10.1016/j.msea.2014.04.077
0921-5093/

reduced the conduction of the thermal flow from the NZ to the surrounding regions. Consequently, not only the exposed time under higher temperature but also the distribution ranges of the softened zones in the HAZ can be effectively reduced. However, for the case of the moderate or high weld heat input [10] and a thick plate joint, these methods proved to be insignificant because of the limitations of the heat conductive capability.

Although various methods have been developed to avoid softening of FSW joints, post-weld heat treatment (PWHT) is considered effective for removing soft zones, particularly for thick plate joints. However, PWHT with solid solution treatment at high temperatures was shown to cause abnormal coarsening of the grains in the NZ, resulting in the property deterioration of the joints [11]. Therefore, a single aging treatment without a solid solution should be the main approach to improve joint properties. Danaf et al. [12] found that increasing the holding time of aging at 175 °C is beneficial for recovering the strength of the FSW joint for 6082 aluminum alloy. Moreover, the grain in the NZ barely exhibited the tendency for abnormal grain growth. Nevertheless, the initial microstructure of the as-welded joint must be considered in the single aging treatment. For example, if the microstructure of a zone in the joint is just at the peak-aging state, high-temperature aging treatment may degrade the property of the joint owing to over-aging effects.

Currently, deep cryogenic treatment (DCT) is mainly used in alloy steels to further modify the microstructure [13]. There are several theories concerning the effects of DCT in published papers. One is the deep cryogenic environment will cause the decreasing of point defects and the increasing of dislocations density in the crystal. Another one is the nearly-complete transformation of retained austenite into martensite in steels. Besides, the elevated internal energy can also promote the fine dispersed carbides precipitation.

While only few works have been conducted for the effect of DCT on the aluminum alloys [14–16]. Chen et al. [17] systematically studied DCT for several aluminum alloys and found that the strength of the DCT sample at room temperature enhances but ductility decreases. The exception is for 6063 aluminum alloy, in which the strength decreases but elongation increases. In addition, numerical simulations proved that the decrement rate of the residual stress is approximately 58% for the DCT of 7050 aluminum alloy [18]. Qian et al. [19] found that the pre-aging effect resulting from DCT promotes the precipitation of the second phases for ZL201 aluminum alloy. In comparison, there are few reports on the application of DCT to FSW joints.

In this study, the effects of PWHT combined with DCT with low-temperature aging were investigated on the FSW joints of 2024-T351 aluminum alloy. The conceivable mechanism of DCT and low-temperature aging treatment are discussed.

2. Experimental procedures

2024-T351 aluminum alloy sheets with a gauge thickness of 2 mm were employed. Their nominal compositions are 4.3% Cu, 1.6% Mg, 0.7% Mn, and the balance Al. Sheets with a width of 60 mm and length of 150 mm were butt welded on an FSW machine (FSW-3LM-2010). The stir tool with a shoulder and pin was made of H13 steel. The diameters of the threaded pin and tool shoulder were 1.9 mm and 10 mm, respectively. The travel and rotational speeds of the tool were 200 mm/min and 1500 rpm, respectively. The tilt angle of the tool was 2°.

Three different treatments were conducted immediately after welding: low-temperature aging (LTA) treatment at 120 °C for 8 h, DCT at −196 °C for 24 h, and DCT combined with low-temperature aging treatment (DCA).

The specimens for metallographic analyses and tensile tests were cut perpendicular to the welding direction using an electrical-discharge cutting machine. The metallographic specimens were polished, etched with 25% nitric acid at 75 °C for ~3 min, and then observed by optical microscopy (Axiovert 200 MAT) and scanning electron microscopy (SEM; HITACHI S-3400). Energy-dispersive spectroscopy (EDS) was employed to identify the composition of the precipitation particles. To investigate the evolution of precipitates in the as- and post-welded treatment joints, differential scanning calorimetry (DSC) was conducted using a NETSCH STA449C DSC instrument. Each specimen, 3 mm in diameter and 1.8 mm in thickness, was heated from 298 K to 823 K at a speed of 20 K/min.

The Vickers microhardness distribution perpendicular to the weld direction was measured on a FM-ARS9000 Vickers hardness instrument with a load of 200 g and an interval of 0.5 mm. The configuration and size of the tensile specimens were prepared with reference to the JIS Z2201 standard, and the tensile tests were performed on a servo-hydraulic mechanical testing system at a tensile speed of 2.4 mm/min. The fracture surfaces were examined by SEM.

3. Results

3.1. Microstructures of the as-welded FSW joints

The metallographic microstructures on the cross section of the as-welded joint are shown in Fig. 1. From the overall observation shown in Fig. 1a, the FSW joint is conventionally divided into four regions, i.e., the NZ, TMAZ, HAZ, and base metal (BM). The larger and elongated grain structures parallel to the rolling direction (see Fig. 1b) in the BM were replaced by a mount of refined grains in the NZ (see Fig. 1c). This is attributed to the dynamic recrystallization caused by severe thermal plastic deformation in the NZ. A mixture of coarsened and refined grains in the TMAZ was typical because of the incomplete dynamic recovery and recrystallization in this zone (see Fig. 1d). The TMAZ is a transitional region between the NZ and HAZ. The width of this transitional region is narrower on the advancing side than on the retreating side. The grain size in the HAZ (see Fig. 1e) was not different from that in the BM. This is because the thermal affection is insufficient to modify the initial grain structure of the HAZ. Normally, the coarsening or dissolving of precipitates causes the major variations in the microstructure of the HAZ. The detailed variations in the microstructures and their effects on the performance of FSW joints are discussed later.

3.2. Hardness distribution

The hardness distributions of the four joints under different treatment states are shown in Fig. 2. In FSW joints of high-strength aluminum alloys, the minima hardness zones are always those in which precipitates occur with notable variation due to the weld heat effect. Under the present welding parameters, although a high peak temperature resulted in high hardness in the NZ, softening was inevitable in the FSW joints. There were two obvious soft regions (labeled I and II in Fig. 2) in the HAZ on both the advanced and retreating sides for the as-welded joint. The same result has been reported by Jones et al. for the FSW joint of 2024-T351 aluminum alloy [2]. These soft zones had almost no variation after post-welded treatment by single DCT. However, after the post-welded LTA treatment at 120 °C for 8 h, soft zone I (SRI) vanished, while the minima hardness in the soft zone II (SRII) increased. Similarly, the hardness in SRI increased in the same way with the post-welded DCA; however, the minima hardness in SRII did not vary with the expected amplitude. This smaller increment implies an effect resulting from DCT prior to LTA.

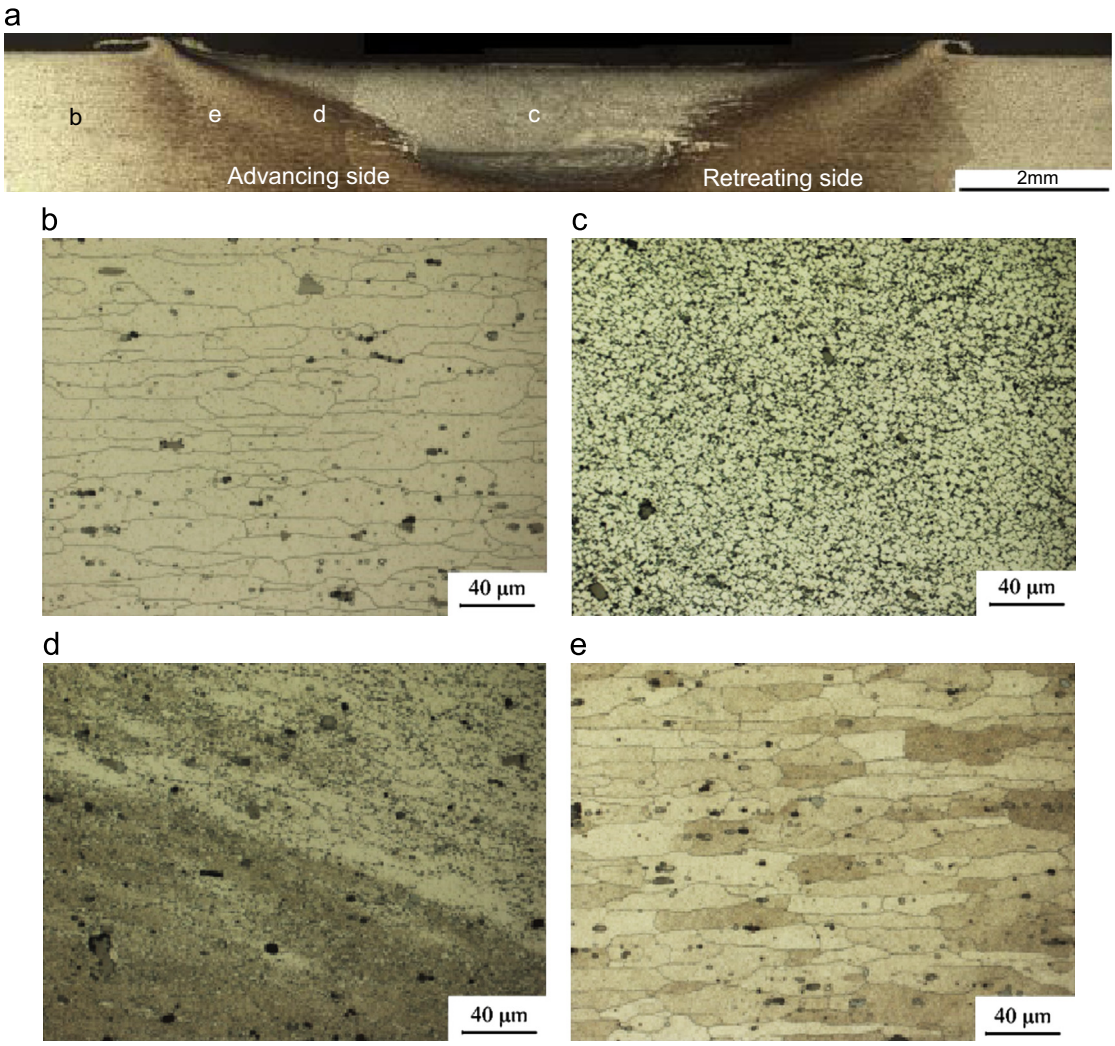

Fig. 1. Metallography on the cross-section of the joints: macrostructure of the joints (a), microstructures of the base metal (b), NZ (c), TMAZ (d) and HAZ (e).

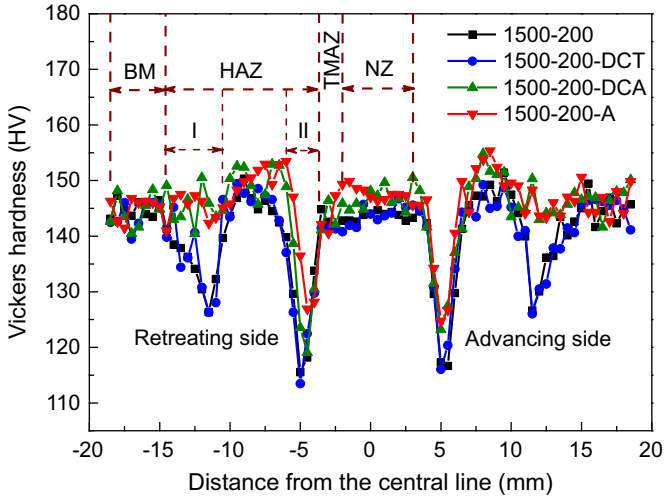

Fig. 2. Hardness distribution of the joints under different treatment conditions.

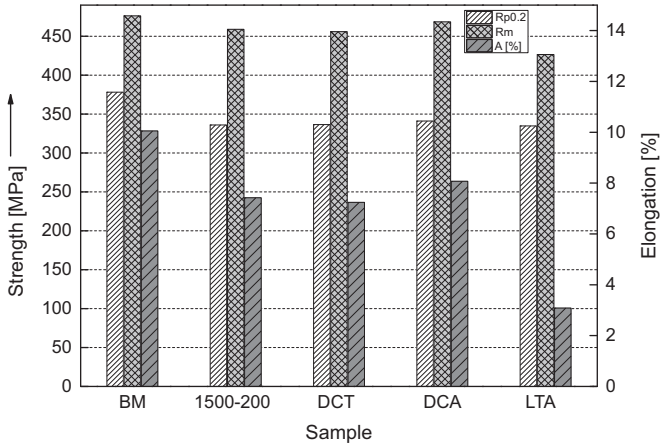

Fig. 3. Comparison of the tensile properties of the joints under different treatment conditions. Rp0.2: yield stress (MPa), Rm: ultimate tensile stress (MPa), A [%]: elongation.

3.3. *Tensile performances*

Fig. 3 shows the comparison of tensile properties among the FSW joints after different post-welded treatments. The UTS of the as-welded joints was 458 MPa, which is 96.3% that of the BM (476 MPa). Meanwhile, elongation was nearly 74% that of the BM. In comparison, both UTS and elongation of the single DCT joint slightly decreased compared with those in the as-welded joint. Similarly, for the single LTA joint, the strength decreased to 426 MPa, which is approximately 90% that of the BM, and the elongation decreased to 38% that of the BM. However, UTS and

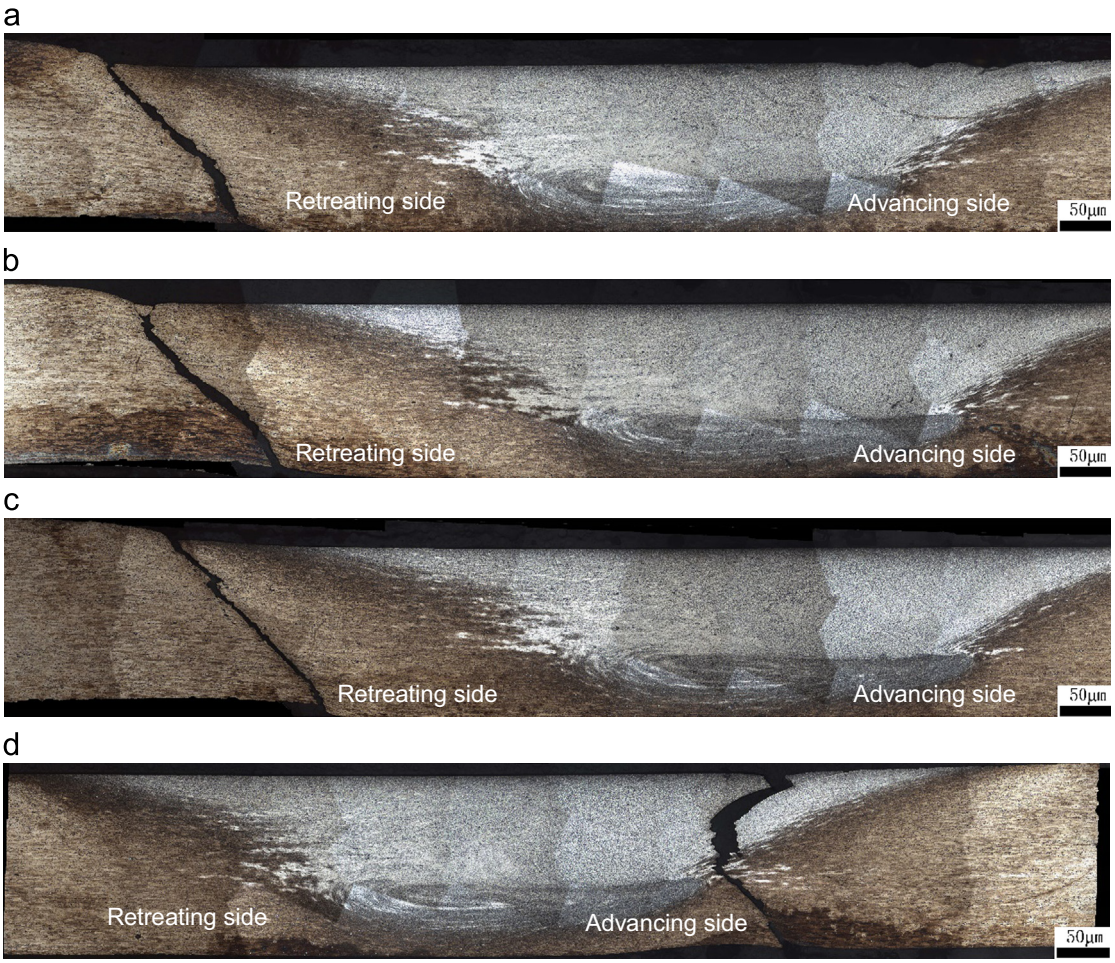

Fig. 4. Fracture locations of the tensile samples for the as-welded joint (a), and joints with DCT (b), DCA (c) and LTA (d).

especially elongation of the DCA joint improved significantly; elongation increased to 80.2% that of the BM.

Fracture location observation results (as shown in Fig. 4) indicate that the as-welded joint (see Fig. 4a), DCT joint (Fig. 4b), and DCA joint (Fig. 4c) fractured at SRII on the retreating side of the joint. The crack path was nearly 45° from the normal direction of the welded plate. This is a typical shearing fracture mode often encountered in the plate tensile test. However, the abnormal fracture occurred at the NZ near the advancing side of the LTA joint. Moreover, the crack feature at the upper position of the NZ was smooth (see Fig. 4d).

Further observations of the fracture surfaces of the above joints are shown in Fig. 5. For the specimens' fracture at SRII on the retreating side of the joint, the fracture surface exhibited similar features, which were composed of cleavage planes and small dimples (see Fig. 5a–c). However, for the specimen fracture at the NZ, a smooth surface feature, which corresponds to the crack position in Fig. 4d, was easily distinguished at the upper position of the fracture surface (see Fig. 5d). We can deduce that this fracture surface may be closely involved with the segregation of the microstructure, particularly the precipitates.

4. Discussions

4.1. Microstructure evolution of soft regions

The hardness distribution of an FSW joint of a heat-treatable strengthening aluminum alloy is close to the variations of the microstructure, which strongly depend on the weld heat input condition. In the HAZ, weld heat often causes grain growth and dissolution or coarsening of precipitates. As a result, softening in the HAZ is inevitable, especially when the GP zones are the main strengthened phase in T351 tempered microstructure of 2024 aluminum alloys.

Fig. 6 shows the DSC analysis results of the precipitates under different post-weld treatments in the SRI. An endothermic peak (labeled I) was observed near 150 °C in the DSC curve, which is attributed to the dissolution of the GPI zone. Another endothermic peak (labeled II) was observed at 240 °C, which is attributed to the dissolution of the unstable phases, such as the GPII zones or the S'' unstable phase. On the other hand, the two endothermic peaks overlap with each other, implying that the structures of the GPI and GPII zones are similar [20]. Based on the calculation of the peak area under the DSC curve, we can deduce the total volume fraction of the GPI and GPII zones before DSC heating, i.e., the as-treated specimens. The larger the area, the greater the volume fraction of the GP zones in the as-treated specimens [21]. The exothermic peak near 270 °C (labeled III) is attributable to the precipitation of the S' or stable S phases. However, the S' phase cannot be easily distinguished from the S phase and thus is regarded as the same as the S phase. Assuming minimal overlapping of endothermic and exothermic heat flows between GP zones transforming to the S phase and the dominance of the formation energy over other factors such as coarsening, the peak area at the region labeled II corresponds to the amount of the S phase transformed at the expense of the GPB zone during the DSC experiment, which is complementary to the amount of the S phase

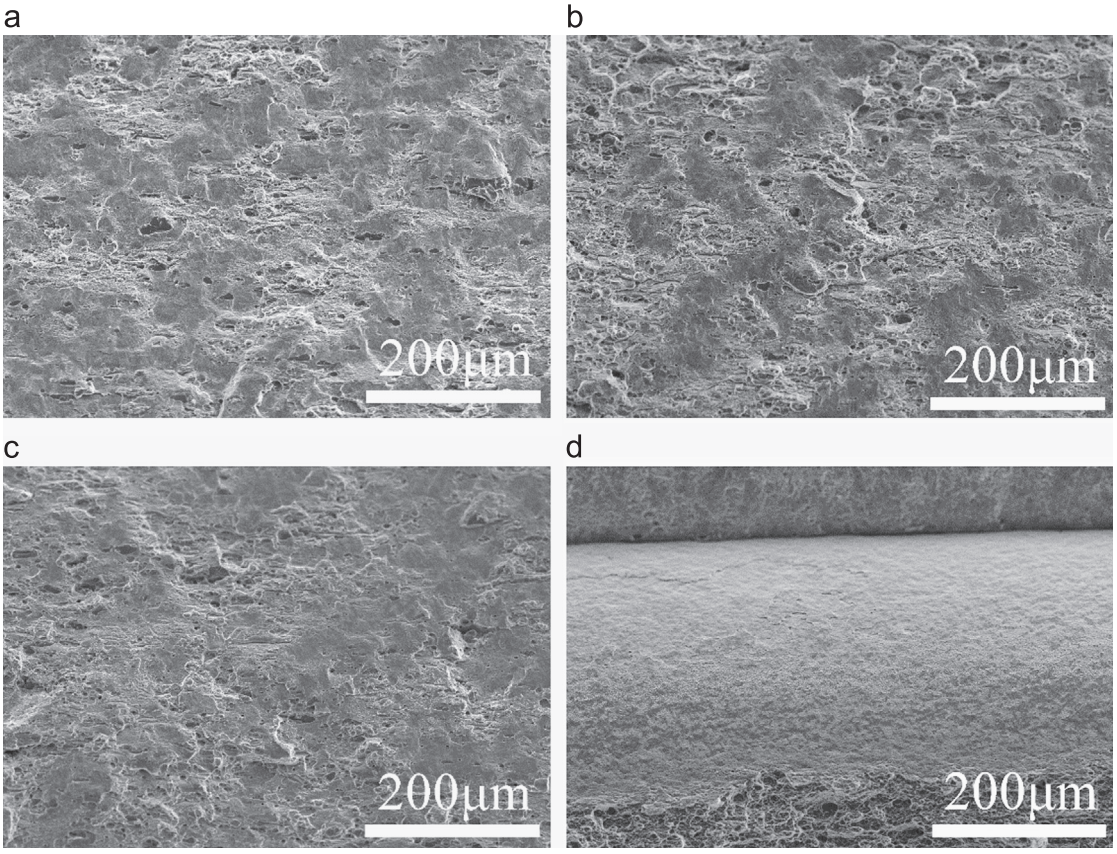

Fig. 5. Fracture surfaces of the tensile samples for the as-welded joint (a), and joints with DCT (b), DCA (c) and LTA (d).

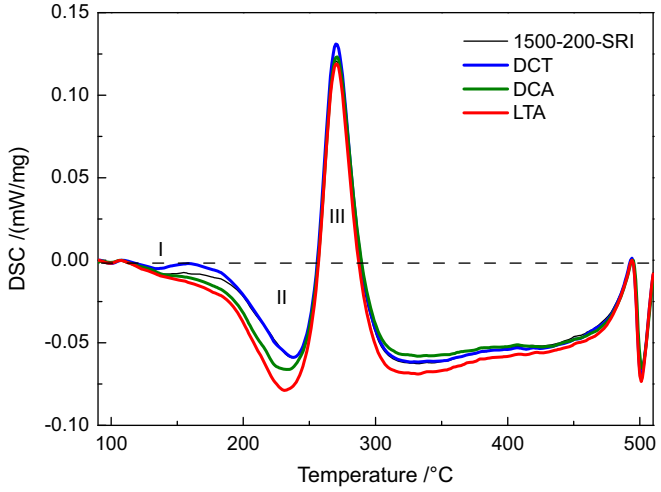

Fig. 6. DSC analysis of the joints in the SRI under different treatment conditions.

originally present in the as-treated sample. That implies that the more *S* is transformed from the GP zones, the less is the amount of the original *S* phase in the as-treated specimens.

The SRI appears possibly as a result of the dissolution of the GP zones or the very fine *S* phase owing to the thermal cycle during the FSW [2]. As shown in Fig. 6, the fractions of the GP zones increase in the specimen treated by DCA and LTA. This is mainly because the LTA at 120 °C facilitates the further precipitation of the GPII zones in the SRI, increasing the hardness in those regions. In comparison, single DCT cannot result in obvious effects on the GP zones. Instead of an increase, a slight decline in the fraction of the GPI zone can be observed for single DCT. We can deduce that single DCT accelerates the re-dissolution of the GPI zones, but such a small infraction of the GPI zone is not sufficient to cause the obvious variation in the hardness of the soft zones. Thus, the disappearance of the SRI in joints should be contributed to the effect of aging at 120 °C during DCA and LTA.

The other regions also present similar results but not as obvious as those in the SRI because of the different initial states. For example, the NZ was found to have typically refined grains with some unstable phases, which can re-precipitate during the cooling stage or natural aging after FSW and result in a higher hardness in the NZ. In addition, the soft mechanism of the SRII has been reported to be the coarsening of the fine *S* phases [2]. In the present LTA or DCA treatment results, the hardness in the NZ slightly increases because of further precipitation of the unstable phases; however, the fraction of the GP zone existing in the SRII is too small to cause an obvious increase in the hardness.

4.2. Tensile fracture behavior

The tensile properties and fracture locations of FSW joints are, to a large extent, dependent on the hardness distribution of the joints. From Fig. 2, both SRI and SRII are the weakening locations of the joints, especially SRII, which has hardness minima in the overall joints irrespective of the treatments employed. Thus, the tensile fracture prefers to occur at the SRII (see Fig. 4a to c). However, it is notable that the fracture location shifts from the SRII to NZ in the case of LTA (see Fig. 4d). Moreover, the crack feature on the upper position of the NZ appears smooth and may be related to the segregation of the precipitates. To seek the causes of this fracture feature, a special etched method was employed to highlight the precipitates in the NZ for joints treated by DCA and LTA.

From the SEM observations in Fig. 7, the features of the segregation bands of the precipitates (shown by arrows) can be easily distinguished in the NZ of all specimens. Fig. 7a shows the

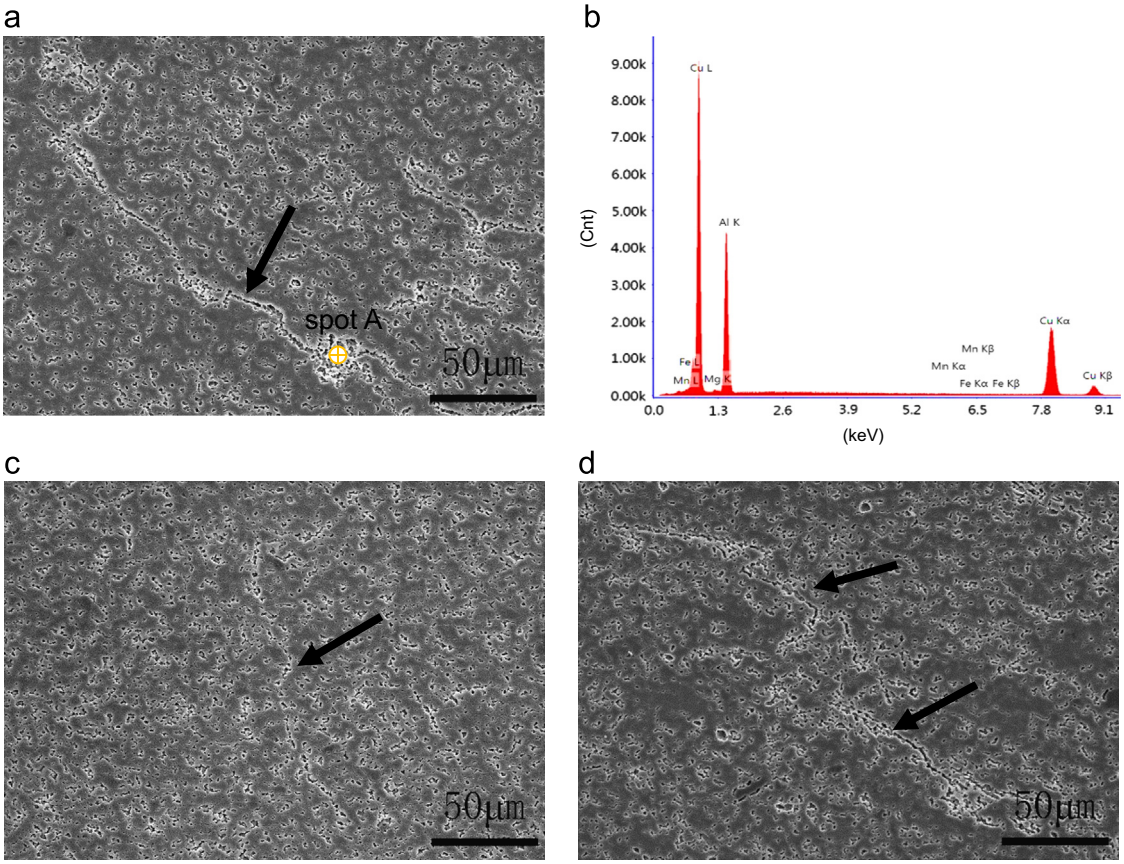

Fig. 7. Observations of the segregation bands in the NZ. (a) The as-welded joint, (b) The EDS results of precipitates located at the spot A as shown in (a), (c) the DCA joint, and (d) the LAT joint.

distribution of precipitates in the as-welded specimen. The EDS results of the precipitates at the point (labeled A in Fig. 7a) on the segregation band indicate that the segregation bands consist of Al–Cu phases (see Fig. 7b). The same results were also obtained by Ma et al. for 2024-T3 alloy FSW joint [22]. The existence of the segregation bands in the NZ can cause a crack along these regions at lower stress levels. Accompanied by grain refinement in the NZ, the precipitates can form segregation bands, which are related to the diffusion of the alloy elements under the cooperative effects of the larger gradient of the strain or strain rate and weld heat during FSW.

After DCA treatment, the segregation bands become thinner and shorter. Meanwhile, the distribution of the precipitates appears to be more dispersed and uniform (Fig. 7c). On the contrary, the more serious segregation can occur in the NZ when treated by a single LTA (Fig. 7d). In fact, the microstructure in the NZ is often considered an incomplete aging state. This indicates that the unstable phase particles will continuously precipitate at moderate thermodynamic conditions after FSW. Therefore, the LTA promotes the precipitation process of the unstable phases at the existing segregation bands. On this account, a pre-DCT was performed before LTA in the process of DCA. The pre-DCT results in shrinking weld volume. Consequently, it leads to the decrease in the vacancy density and increase in the dislocation density. The above processes effectively weaken the segregation extent in the NZ during the subsequent LTA. The detailed processes can be explained as follows: the compressive strain resulting from the lattice shrink may lead to the re-precipitation or re-dissolution of unstable precipitates with coherent or semi-coherent lattices in the matrix. These processes may also occur at the regions near the segregation bands. This may not only reduce the tendency of the solute atoms to migrate to the segregation bands but also promote the dispersed precipitation of the unstable phases in the matrix during subsequent LTA. On the other hand, the dislocation density increases because of the lattice shrink at cryogenic temperatures. This results in enhanced interaction between the vacancies and dislocations. Meanwhile, the long distance diffusion of a single solute atom is difficult under the present aging temperature condition, and the solute atom and vacancy prefer to constitute a diffusion couple. Thus, the migration of the solute atoms largely depends on the diffusion capability of the vacancies. In the subsequent LTA process, although lattice expansion occurs, resulting in the regeneration of the vacancies, the solute atom–vacancy diffusion couples cannot migrate a long distance because of high-density dislocations. However, these diffusion couples can easily migrate to the segregation bands since there are few dislocation obstacles after dynamic recrystallization in the single LTA NZ. Consequently, the overall tensile performance of the FSW joint treated by the DCA improves.

5. Conclusions

(1) Two types of soft regions exist in the HAZ of the as-welded joint: SRI and SRII. Both DCA and LAT can remove the SRI, but not the SRII, with the minima hardness.
(2) After treatment by the single LTA, the elongation of the as-welded joint dramatically decreased and was accompanied by a small decrement in the strength. The tensile fracture location shifted from the SRII of the as-welded joint to the NZ of the LTA joint. This indicated that a single LTA does not improve the tensile property of the as-welded joint but deteriorates it. However, an enhanced tensile property was achieved using DCA, in which a pre-DCT was employed before the LTA.

Meanwhile, the fracture at the segregation bands in the NZ was inhibited.

(3) The effects of the DCA on the mechanical performance of the joint can be summarized as follows: pre-DCT promotes the re-dissolution or dispersed precipitation of the unstable phases in the as-welded joints. However, the pre-DCT can retard the migration of the atom–vacancy couples toward the segregation bands in the NZ because of an increase in the dislocation obstacles. Finally, the tensile fracture along the segregation bands that occurred in the single LTA joint was inhibited.

Acknowledgments

The authors thank the China Friction Stir Welding Center, Beijing Friction Stir Welding Technology Limited Company for financial support.

References

[1] R.S. Mishra, Z.Y. Ma, Mater. Sci. Eng. Rep. 50R (2005) 1–78.
[2] M.J. Jones, P. Heurtier, C. Desrayaud, F. Montheillet, D. Alléhaux, J.H. Driver, Scr. Mater. 52 (2005) 693–697.
[3] K.A. Hassan, P.B. Prangnell, Sci. Technol. Weld. Join. 8 (2003) 257–268.
[4] A.P. Reynolds, W. Tang, Z. Khandkar, Sci. Technol. Weld. Join. 10 (2005) 190–199.
[5] R.D. Fu, J.F. Zhang, Y.J. Li, J. Kang, H.J. Liu, F.C. Zhang, Mater. Sci. Eng. A 559 (2012) 319–324.
[6] P. Upadhyay, A.P. Reynolds, Mater. Sci. Eng. A 527 (2010) 1537–1543.
[7] L. Fratini, G. Buffa, R. Shivpuri, Int. J. Adv. Manuf. Technol. 43 (2009) 664–670.
[8] R.D. Fu, Z.Q. Sun, R.C. Sun, Y. Li, H.J. Liu, L. Liu, Mater. Des. 32 (2011) 4825–4831.
[9] S. Benavides, Y. Li, L. Murr, Scr. Mater. 41 (1999) 809–815.
[10] L. Fratini, G. Buffa, R. Shivpuri, Acta Mater. 58 (2010) 2056–2067.
[11] H. Aydın, A. Bayram, I. Durgun, Mater. Des. 31 (2010) 2568–2577.
[12] E.A. El-Danaf, M.M. El-Rayes, Mater. Des. 46 (2012) 561–572.
[13] Y. Dong, X.P. Lin, H.S. Xiao, Heat Treat. Met. (UK) 25 (1998) 55–59.
[14] J.J. Wang, X.D. Xue, Z.Q. Yang, H. Zhang, Y. Zhou, Adv. Mater. Res. 146 (2011) 1646–1650.
[15] H. Zhang, J. Wang, J. Guo, HWT 20 (2009) 41–45 (in Chinese).
[16] F. Bouzada, M. Cabeza, P. Merino, S. Trillo, Adv. Mater. Res. 445 (2012) 965–970.
[17] D. Chen, W.X. Li, TNMSC 10 (2000) 891–895 (in Chinese).
[18] J. Fu, Q.C. Wang, X.D. Hu, LTSG 2 (2005) 6–8 (in Chinese).
[19] S.Q. Qian, M.P. Li, M.J. Yan, J. Xu, J. Shanghai Univ. Eng. Sci. 4 (2001) 257–262.
[20] C. Genevois, A. Deschamps, A. Denquin, B. Doisneau-Cottignies, Acta Mater. 53 (2005) 2447–2458.
[21] V. Dixit, R.S. Mishra, R.J. Lederich, R. Talwar, Sci. Technol. Weld. Join. 14 (2009) 346–355.
[22] Z. Zhang, B.L. Xiao, Z.Y. Ma, Metall. Mater. Trans. A 44 (2013) 4081–4097.